



Published in final edited form as:

Soft Matter. 2014 April 14; 10(14): 2372–2380. doi:10.1039/c3sm52265b.

Three-dimensional patterning of multiple cell populations through orthogonal genetic control of cell motility

Joanna L. MacKay^a, Anshum Sood^b, and Sanjay Kumar^c

Sanjay Kumar: skumar@berkeley.edu

^aDepartment of Chemical and Biomolecular Engineering, University of California-Berkeley, Berkeley, California 94720, USA

^bDepartment of Bioengineering, University of California-Berkeley, Berkeley, California 94720, USA

^cDepartment of Bioengineering, University of California-Berkeley, Berkeley, California 94720, USA. Fax: 510-642-5835; Tel: 510-643-0787

Abstract

The ability to independently assemble multiple cell types within a three-dimensional matrix would be a powerful enabling tool for modeling and engineering complex tissues. Here we introduce a strategy to dynamically pattern distinct subpopulations of cells through genetic regulation of cell motility. We first describe glioma cell lines that were genetically engineered to stably express constitutively active or dominant negative Rac1 GTPase mutants under the control of either a doxycycline-inducible or cumate-inducible promoter. We culture each population as multicellular spheroids and show that by adding or withdrawing the appropriate inducer at specific times, we can control the timing and extent of Rac1-dependent cell migration into three-dimensional collagen matrices. We then report results with mixed spheroids in which one subpopulation of cells expresses dominant negative Rac1 under a doxycycline-inducible promoter and the other expresses dominant negative Rac1 under a cumate-inducible promoter. Using this system, we demonstrate that doxycycline and cumate addition suppress Rac1-dependent motility in a subpopulation-specific and temporally-controlled manner. This allows us to orthogonally control the motility of each subpopulation and spatially assemble the cells into radially symmetric three-dimensional patterns through the synchronized addition and removal of doxycycline and cumate. This synthetic biology-inspired strategy offers a novel means of spatially organizing multiple cell populations in conventional matrix scaffolds and complements the emerging suite of technologies that seek to pattern cells by engineering extracellular matrix properties.

Introduction

Virtually all tissues are composed of a diversity of cell populations that are spatially organized into complex structures. For example, arteries and arterioles contain ordered layers of endothelial and smooth muscle cells, aveoli consist of closely apposed epithelial

and endothelial monolayers, and many nerves include neuronal axons tightly ensheathed by Schwann cells. Even multicellular systems that are initially homogenous, such as pluripotent stem cell colonies, can spontaneously develop patterns over time as physicochemical gradients form and specific subpopulations grow, die, and differentiate.¹⁻³ Importantly, loss of tissue architecture is a central hallmark of cancer, and providing the organizational cues associated with normal tissue may help “revert” malignant cells to a quiescent phenotype.⁴⁻⁶ In an effort to recreate such organizational complexity in vitro, many approaches have been developed to spatially pattern cells by engineering extracellular matrix (ECM) properties. For example, ECM proteins can be patterned in two-dimensional cultures using stamping, writing, or photolithographic approaches to create adhesive areas of different shapes and sizes.⁷⁻⁹ Lithographic methods can also be used to create topographical features in ECM, such as wells for capturing cells or ridges for cell alignment.^{10, 11} Additionally, there is now a growing toolbox for organizing cells within three-dimensional scaffolds, including light-based patterning of ECM stiffness and adhesion^{12, 13} and molding scaffolds around three-dimensional printed structures.¹⁴⁻¹⁹ An important motivation of many of these approaches is to position specific cell types at specific locations within the scaffold, with an eye towards engineering functional tissues or creating organotypic models that may be exploited for mechanistic discovery and screening.

While these approaches have proven quite powerful, they all share the need for custom-engineered materials, which may require significant user skill to manufacture or be imperfectly suited to a given biomedical application. Moreover, while innovative methods are beginning to emerge that enable dynamic pattern modulation in the presence of cells,²⁰⁻³⁴ the majority of matrix engineering strategies create patterns that are “hard-wired” into the material. One can envision that an alternative but complementary approach to this family of technologies could be to instruct cells to pattern themselves, for example by directly regulating their migration through manipulation of intracellular signaling pathways. Indeed, Rac1 GTPase would be a prime molecular target since it stimulates actin polymerization at the leading edge of migrating cells³⁵, and previous studies have shown that inhibiting Rac1 suppresses the motility of various cell types such as fibroblasts,^{36, 37} glioma cells,³⁸⁻⁴⁰ lung carcinoma cells,^{41, 42} and breast cancer cells.⁴³⁻⁴⁵ Therefore dynamically altering Rac1 activity in motile cells could provide control over the extent of cell migration within an ECM and potentially facilitate the spatial positioning of cells.

Dynamic control over Rac1 activity has previously been achieved using a Rac1 mutant genetically engineered to be photoactivatable, such that blue light illumination reversibly uncages and activates the protein.⁴⁶ By expressing this mutant in HeLa cells, it was possible to initiate cell migration in a particular direction by illuminating one edge of the cell.⁴⁶ While this provides a powerful and highly innovative technique for temporal and spatial control over cell motility, the reversible nature of the photoactivatable mutant requires that a cell be repeatedly illuminated every few minutes to continuously stimulate migration.⁴⁷ Since simultaneously illuminating many selected cells in a matrix scaffold while leaving others unperturbed would presumably be challenging, photopatterning multiple cells within a three-dimensional ECM and maintaining those patterns for long periods of time would likely be difficult.

It occurred to us that another method to temporally control Rac1 activity could be to express genetic mutants from conditional promoters, as we had done to vary the activity of RhoA and myosin light chain kinase in a previous study.⁴⁸ Various promoter systems have been developed for use in mammalian cells that induce expression in response to antibiotics,^{49–53} steroid hormones,^{54–56} and metabolites.^{57–59} While the requirement for transcription and translation renders the induction kinetics of these approaches significantly slower than for photoactivatable proteins, these promoter systems provide reversible and stable control over protein activity within an entire population of cells, by simply adding or removing the transcriptional inducer. Furthermore, several studies have shown that by combining two or three promoters into the same cell, the expression of multiple genes can be orthogonally controlled.^{51, 52, 60, 61} This suggests that the migration of multiple populations of cells could be manipulated in a similarly orthogonal manner by introducing a different promoter system into each population to drive expression of Rac1 mutants.

In this study, we demonstrate that we can independently control the motility of multiple cell populations in either homogeneous or heterogeneous cultures by expressing genetic mutants of Rac1 under mutually orthogonal promoter systems induced by doxycycline⁶² or cumate.⁵⁹ We show that either promoter system can be used to control the timing and extent of cell migration from multicellular spheroids within three-dimensional matrices by turning expression of the Rac1 mutants on and off. This in turn allows us to mix cells expressing the doxycycline-inducible promoter with cells expressing the cumate-inducible promoter and to spatially pattern the two subpopulations into radially symmetric three-dimensional patterns.

Experimental methods

Cell lines and reagents

CA Rac1 (Q61L)⁶³ and DN Rac1 (T17N)⁶⁴ were first subcloned into the entry vector pEN_TTmcs⁶², which contains the TRE-tight doxycycline-inducible promoter. Gateway recombination was then used to transfer the promoter and Rac1 genes into the lentiviral destination vector pSLIK-Venus⁶², containing the reverse tetracycline transactivator (rtTA) and the yellow fluorescent protein (YFP) variant Venus. pENTT_mcs and pSLIK Venus were originally obtained from the American Tissue Culture Collection (ATCC, Manassas, VA), but are now available through the Addgene repository as plasmid # 25755 and plasmid # 25734. CA Rac1 and DN Rac1 were also subcloned into the lentiviral SparQ expression vector (QM516B-1, System Biosciences, Mountain View, CA) containing the cumate-inducible promoter,⁵⁹ puromycin resistance, and red fluorescent protein (RFP). The cumate-inducible promoter system also requires expression of the cumate repressor (CymR) from a separate lentiviral vector (QM400PA/VA-1, System Biosciences) that confers neomycin resistance. Viral particles were packaged in HEK 293T cells (ATCC) as previously described.⁶⁵ U373-MG human glioma cells (ATCC HTB-17) were obtained from the Tissue Culture Facility at the University of California, Berkeley and were transduced at a multiplicity of infection of 1 IU/cell for the pSLIK vector and 3 IU/cell for both the SparQ and CymR expression vectors. Cells expressing the pSLIK vector were sorted on a DAKO-Cytomation MoFlo High Speed Sorter based on Venus fluorescence, and cells expressing the SparQ and CymR vectors were selected in 1 µg/ml puromycin (Sigma-Aldrich, St.

Louis, MO) and 400 µg/ml G418 (Sigma-Aldrich) for two weeks. Control cell lines were created in the same manner with empty vectors. U373-MG cell lines were maintained at 37°C in a 5% CO₂ humidified chamber and cultured in high glucose DMEM (Life Technologies, Carlsbad, CA) supplemented with 10% calf serum (J R Scientific, Woodland, CA), 100 U/ml penicillin, 100 µg/ml streptomycin, 1x MEM non-essential amino acids, and 1 mM sodium pyruvate (all Life Technologies). To induce gene expression from the pSLIK vector, 25 ng/ml doxycycline (Fisher Bioreagents, Waltham, MA) was added to the cell culture medium. To induce gene expression from the SparQ vector, 12 µg/ml cumate (System Biosciences) was added. Cells expressing the pSLIK vectors were labeled with the green cytoplasmic dye CMFDA (Life Technologies, Carlsbad, CA) before experiments, because the Venus fluorescence alone was too dim to track cells over multiple days.

Spheroid invasion assay

Spheroids of approximately 200 cells were created by culturing droplets of cells upside down in a culture dish for 3–4 days.^{66–68} The spheroids were then collected and suspended within a 1 mg/ml solution of bovine collagen I (PureCol, Advanced BioMatrix (San Diego, CA)) diluted with culture medium, which was allowed to gel for 1 hour at 37°C before additional medium was added. For experiments in which doxycycline/cumate was later added or removed, all gels (including controls in which the inducer concentration remained constant) were washed 6 times with each wash consisting of a 30-minute incubation in fresh medium. Live phase contrast and epifluorescence imaging were performed using a Nikon Ti-E microscope (Nikon Corporation, Tokyo, Japan) to acquire images near the midplane of each spheroid. To measure the migration of cells that had protruded or migrated out of the spheroid, the distance between the cell position and the center of the spheroid was manually measured using ImageJ. The original radius of the spheroid was subtracted from these distance measurements to estimate the distance over which each cell had migrated. In Figure 4, the epifluorescence images for each condition were overlaid to create a “heat map” by using the built-in Z-project function in ImageJ to select the maximum intensity value of each pixel for the red channel (RFP, displayed as magenta) and the green channel (Venus + CMFDA) separately.

Statistical analysis

The migration distances were compared between samples in which doxycycline/cumate was added or removed using a Welch’s t-test with *n* equal to the number of cells in each condition, which increased over time as more cells migrated into the surrounding matrix. To convey changes in migration over time, the migration distances versus time were fit for all cells in a given condition using linear least squares regression separately for the time period before media changes (*t* = 24 h or *t* = 48 h) and after (*t* = 24 h or *t* = 48 h). The slopes ± standard error (s.e.) from the linear regression calculations were compared between media conditions using a Student’s t-test.

Results and discussion

As initial proof of principle, we first sought to create cell lines in which we could control cell motility by introducing a single migration-relevant gene under the control of a small-

molecule inducer. We chose Rac1 GTPase as a target, given the central role this molecule has been shown to play in lamellipodial protrusion and directional cell migration.^{35, 36} To override endogenous feedback, we cloned constitutively active (CA) or dominant negative (DN) mutants of Rac1 GTPase into lentiviral vectors in which gene expression is controlled by either a doxycycline-inducible promoter or a cumate-inducible promoter. We then transduced U373-MG human glioma cells with these vectors to yield stable cell lines. Previously, we and others have shown that when multicellular spheroids composed of naïve glioma cells are implanted into a three-dimensional collagen gel, individual cells actively invade the surrounding matrix over several days.^{66, 67, 69–72} To confirm that altering Rac1 activity affects this type of 3D motility, we cultured each of our four cell lines (doxycycline- and cumate-inducible DN and CA Rac1) or empty vector control cells as spheroids in the presence of doxycycline or cumate for several days to induce expression of the mutant genes. We then implanted the spheroids into collagen I gels still in the presence of doxycycline or cumate and tracked their invasion over time (Fig. 1). We found that CA Rac1 expression from either promoter caused a dramatic increase in cell migration into the surrounding matrix. These cells were more elongated than control cells, and they exerted multiple dynamic processes presumably associated with engagement and remodeling of the collagen matrix. In contrast, DN Rac1 expression almost completely abolished cell motility, resulting in more compact spheroids with very few migrating cells. This is consistent with previous studies showing that Rac1 is necessary for glioma cell migration through 3D matrices.^{38–40, 73}

Recognizing that expression of DN Rac1 could be used as a “stop” signal to suppress cell migration, we investigated whether we could temporally control cell migration by dynamically switching expression of DN Rac1 on and off. First, we cultured the doxycycline-inducible DN Rac1 cells as spheroids in the absence of doxycycline and allowed them to invade the collagen gel for 24 hours. We then changed the culture medium to either add doxycycline to induce DN Rac1 expression or to remain without doxycycline, as a control. We found that two days later, the invasion patterns of spheroids in which doxycycline was added had not changed over time, while the spheroids without doxycycline continued to invade into the surrounding matrix. This indicated that cell migration was suppressed within 2 days of inducing DN Rac1 expression, which we quantified by measuring the average distance that cells had migrated away from the spheroids (Fig. 2A). This showed that 48 hours after doxycycline addition ($t = 72$ h), cells without doxycycline had migrated significantly farther than cells for which doxycycline was added. To more clearly visualize these changes in cell migration, we superimposed linear fits onto the data, which show that the slope (distance/time) decreased significantly after adding doxycycline (Fig. 2C). The slope of cell distance/time for spheroids remaining without doxycycline also decreased after changing the medium, but to a lesser degree, which could be due to changes in the intrinsic motility of cells over time as spheroidal cell-cell contacts are broken and cell-matrix contacts are formed or to refreshment of motility-regulating factors after changing the culture medium. To determine whether DN Rac1-suppression of cell migration was reversible, we also cultured the cells as spheroids with doxycycline, implanted them into collagen, and then removed doxycycline 48 hours later through repeated medium changes. We found that cells began migrating into the surrounding gel within 24 hours of removing

doxycycline ($t = 72$ h), and significant invasion had occurred by the next day (Fig. 2B and 2C). For comparison, we also cultured spheroids continuously in doxycycline and found that these spheroids remained relatively compacted throughout the four day experiment with few migrating cells. We repeated these experiments with cells expressing cumate-inducible DN Rac1 and saw similar effects upon adding and removing cumate, both in their qualitative migration behavior and in their measured migration distance (Fig. 3).

After demonstrating that we could manipulate the timing and extent of cell migration by regulating DN Rac1 expression from either promoter system, we investigated whether we could mix the two populations of cells into the same spheroid and independently control their migration in order to spatially pattern the cells. To accomplish this, we combined equal numbers of cells expressing either cumate-inducible or doxycycline-inducible DN Rac1, cultured them as spheroids in the presence of either doxycycline or cumate, and tracked their migration through collagen gels. We used epifluorescence imaging to visually distinguish the two populations, since the cumate-inducible vector encodes a cytoplasmic RFP and the doxycycline-inducible vector encodes a cytoplasmic Venus (YFP variant). We found that when the spheroids were cultured in the presence of doxycycline, the doxycycline-inducible DN Rac1 cells did not significantly migrate into the surrounding collagen, while the cumate-inducible DN Rac1 cells did migrate (Fig. 4A, 4E “Dox Always”). This created a “bullseye” pattern with doxycycline-inducible DN Rac1 cells in the middle surrounded by a ring of cumate-inducible DN Rac1 cells (Fig. 4A). The migration behaviors of both cell types were similar to their behaviors when cultured as homogeneous spheroids, including cell morphology and migration distances over time (compare to Fig. 2B “Dox Always” for doxycycline-inducible DN Rac1 and Fig. 3A “No Cumate” for cumate-inducible DN Rac1). If the spheroids were instead cultured in the presence of cumate, only the doxycycline-inducible DN Rac1 cells migrated (Fig. 4C, 4F “Cumate Always”), producing the opposite fluorescence pattern of cells (Fig. 4C). Again, the migration behaviors of both cell types were similar to their behaviors in homogeneous spheroids (Fig. 2A “No Dox” for doxycycline-inducible DN Rac1, Fig. 3B “Cumate Always” for cumate-inducible DN Rac1), indicating that in the heterogeneous spheroids, the presence of motile cells does not alter the migration of non-motile cells, and vice versa. These results confirm that the doxycycline- and cumate-inducible promoters operate in a mutually orthogonal fashion and that they can be used to independently manipulate the migration of each subpopulation.

Using this same paradigm, we also explored whether we could dynamically change the “bullseye” pattern by switching the transcriptional inducers after two days, and thus the migratory behavior of the two subpopulations. We found that upon changing the inducer from doxycycline to cumate, the doxycycline-inducible DN Rac1 cells began to migrate, while the cumate-inducible CA Rac1 cells slowed down (Fig. 4E). Within three days of the inducer switch, the doxycycline-inducible DN Rac1 cells had effectively caught up with the cumate-inducible DN Rac1 cells, creating a heterogeneous ring of migrated cells (Fig. 4B). This is shown quantitatively in the plot of average migration distance over time, which reveals that the two populations converge at $t = 120$ h (Fig. 4E “Dox to Cumate”). We observed a similar change in pattern with spheroids that were first cultured in cumate for two days and then switched to doxycycline (Fig. 4D and 4F “Cumate to Dox”). In both cases, the migration behaviors of the doxycycline-inducible and cumate-inducible DN Rac1

cells upon adding or removing inducer were strikingly similar to their behavior in homogeneous spheroids (compare Fig. 4E to Fig. 2B “Dox Removed”/Fig. 3A “Cumate Added”, and compare Fig. 4F to Fig. 2A “Dox Added”/Fig. 3B “Cumate Removed”). This further demonstrates our ability to independently control the migration of specific cell populations in a time dependent manner.

This genetic strategy of modulating the intrinsic motility of two populations of cells through mutually orthogonal expression of DN Rac1 allowed us to assemble cells into radially symmetric patterns that we could dynamically change. In the future, one could imagine complementing this cell-intrinsic patterning with other patterning schemes to obtain even greater spatial control. For example microfluidics could be used to create gradients of doxycycline and cumate and thereby vary DN Rac1 expression spatially throughout the culture.⁷⁴ Such flow-based gradients could also be dynamically altered in order to switch inducer concentration or gradient direction.^{75, 76} One could also utilize caged variants of doxycycline that can be irreversibly uncaged with UV light to stimulate doxycycline-inducible gene expression in specific cells.^{77, 78} This method has been used to create cell patterns both in 3D tissue extracts and in vivo using two-photon microscopy.⁷⁹ To impose additional control over the direction of cell migration, one could use materials engineering techniques, such as soft lithography, photolithography or 3D printing, to introduce physical cues into the ECM. For example, tracks of adhesive ligands^{24–28, 80, 81} or topographical channels^{27–30, 82} could be used to steer cells to specific locations. In addition, the matrix stiffness could be patterned to stimulate directional migration through durotaxis.^{31–34, 83–86} Thus combining external patterning techniques with our ability to both start and stop cell migration through temporal control of Rac1 activity would provide a unique opportunity to assemble cells into complex 3D structures that can be dynamically altered over time.

In this study, we used two inducible promoters to demonstrate orthogonal control over the migration of two populations of glioma cells, but this strategy could in theory be extended to include any number of promoter systems as long as they operate in a mutually independent fashion. Previous studies have shown that the following combinations of inducible promoters can be used orthogonally in mammalian cells: tetracycline/ streptogramin,⁵¹ tetracycline/ streptogramin/ macrolide,⁵² and tetracycline/ IPTG.⁶⁰ This suggests that it would be possible to simultaneously control at least five distinct populations of cells. Furthermore, we expect that many other cell types could be similarly manipulated through DN Rac1 expression given previous studies showing that Rac1 plays a dominant role in mesenchymal cell motility.^{36–45} For cell types that exhibit amoeboid motility, which seems to be contractility driven and insensitive to Rac1 manipulation (e.g., leukocytes and some cancer cells), expressing mutants of RhoA GTPase might permit similar temporal control over cell migration.^{87, 88}

In addition to providing a new handle through which to spatially pattern cells, we expect that our genetic approach for manipulating cell motility will be useful for studying biological processes that involve the migration of multiple cell types. During tumor metastasis, for example, cancer cells are able to migrate and metastasize to other parts of the body with the help of various cell types in the tumor stroma, including fibroblasts and macrophages.^{89, 90} In addition, patterning of the human embryo occurs through several coordinated movements

of cells, including gastrulation, neurulation, and neural crest cell migration.^{90, 91} Wound healing also involves the migration of multiple cell types, including the recruitment of immune cells and fibroblasts to the site of injury and the collective migration of keratinocytes and epidermal stem cells to regenerate the epidermis.⁹² Therefore, the ability to independently control the motility of several different populations of cells would provide a powerful experimental tool for studying multicellular aspects of cell migration.

Conclusions

We have demonstrated that cell motility can be choreographed in three-dimensional scaffolds through the inducible expression of genetic mutants of Rac1 GTPase. We show that by combining cell populations in which dominant negative Rac1 expression is controlled by mutually orthogonal promoter systems, we can independently regulate the migration of each population in a temporally coordinated fashion. This study provides a novel tool for controlling multicellular interactions and demonstrates proof-of-principle that cells can be spatially patterned within a 3D matrix by manipulating their intrinsic motility.

Acknowledgments

We thank D.V. Schaffer for valuable technical guidance and for sharing equipment. FACS was performed with the help of H. Nolla and A. Valeros in the Flow Cytometry Facility at the University of California, Berkeley. This work was supported by grants to S.K. from the NSF (1055965, CMMI CAREER Award) and the NIH (1R21EB016359; 1DP2OD004213, Director's New Innovator Award, part of the NIH Roadmap for Medical Research; 1U54CA143836, Physical Sciences Oncology Center Grant).

Notes and references

1. Rogers KW, Schier AF. *Annu Rev Cell Dev Biol.* 2011; 27:377–407. [PubMed: 21801015]
2. Kicheva A, Cohen M, Briscoe J. *Science.* 2012; 338:210–212. [PubMed: 23066071]
3. Nelson CM. *AICHE J.* 2012; 58:3608–3613.
4. Nelson CM, Bissell MJ. *Annu Rev Cell Dev Biol.* 2006; 22:287–309. [PubMed: 16824016]
5. Kumar S, Weaver VM. *Cancer Metastasis Rev.* 2009; 28:113–127. [PubMed: 19153673]
6. Ingber DE. *Semin Cancer Biol.* 2008; 18:356–364. [PubMed: 18472275]
7. Whitesides GM, Ostuni E, Takayama S, Jiang X, Ingber DE. *Annu Rev Biomed Eng.* 2001; 3:335–373. [PubMed: 11447067]
8. Schiele NR, Corr DT, Huang Y, Raof NA, Xie Y, Chrisey DB. *Biofabrication.* 2010; 2:032001. [PubMed: 20814088]
9. Thery M. *J Cell Sci.* 2010; 123:4201–4213. [PubMed: 21123618]
10. Flemming RG, Murphy CJ, Abrams GA, Goodman SL, Nealey PF. *Biomaterials.* 1999; 20:573–588. [PubMed: 10213360]
11. Gomez EW, Nelson CM. *Methods Mol Biol.* 2011; 671:107–116. [PubMed: 20967625]
12. Aizawa Y, Owen SC, Shoichet MS. *Prog Polym Sci.* 2012; 37:645–658.
13. Burdick JA, Murphy WL. *Nat Commun.* 2012; 3:1269. [PubMed: 23232399]
14. Barron JA, Spargo BJ, Ringeisen BR. *Appl Phys A.* 2004; 79:1027–1030.
15. Nahmias Y, Schwartz RE, Verfaillie CM, Odde DJ. *Biotechnol Bioeng.* 2005; 92:129–136. [PubMed: 16025535]
16. Othon CM, Wu X, Anders JJ, Ringeisen BR. *Biomed Mater.* 2008; 3:034101. [PubMed: 18689930]
17. Wu W, Hansen CJ, Aragon AM, Geubelle PH, White SR, Lewis JA. *Soft Matter.* 2010; 6:739–742.

18. Ovsianikov A, Gruene M, Pflaum M, Koch L, Maiorana F, Wilhelmi M, Haverich A, Chichkov B. *Biofabrication*. 2010; 2:014104. [PubMed: 20811119]
19. Miller JS, Stevens KR, Yang MT, Baker BM, Nguyen DH, Cohen DM, Toro E, Chen AA, Galie PA, Yu X, Chaturvedi R, Bhatia SN, Chen CS. *Nat Mater*. 2012; 11:768–774. [PubMed: 22751181]
20. Nakanishi J, Kikuchi Y, Inoue S, Yamaguchi K, Takarada T, Maeda M. *J Am Chem Soc*. 2007; 129:6694–6695. [PubMed: 17488076]
21. Kikuchi Y, Nakanishi J, Shimizu T, Nakayama H, Inoue S, Yamaguchi K, Iwai H, Yoshida Y, Horiike Y, Takarada T, Maeda M. *Langmuir*. 2008; 24:13084–13095. [PubMed: 18925763]
22. Kikuchi Y, Nakanishi J, Nakayama H, Shimizu T, Yoshino Y, Yamaguchi K, Yoshida Y, Horiike Y. *Chem Lett*. 2008; 37:1062–1063.
23. Vignaud T, Galland R, Tseng Q, Blanchoin L, Colombelli J, Thery M. *J Cell Sci*. 2012; 125:2134–2140. [PubMed: 22357956]
24. Lee SH, Moon JJ, West JL. *Biomaterials*. 2008; 29:2962–2968. [PubMed: 18433863]
25. Hoffmann JC, West JL. *Soft Matter*. 2010; 6:5056–5063.
26. DeForest CA, Polizzotti BD, Anseth KS. *Nat Mater*. 2009; 8:659–664. [PubMed: 19543279]
27. DeForest CA, Anseth KS. *Nat Chem*. 2011; 3:925–931. [PubMed: 22109271]
28. Kloxin AM, Kasko AM, Salinas CN, Anseth KS. *Science*. 2009; 324:59–63. [PubMed: 19342581]
29. Sarig-Nadir O, Livnat N, Zajdman R, Shoham S, Seliktar D. *Biophys J*. 2009; 96:4743–4752. [PubMed: 19486697]
30. Iina O, Bakker GJ, Vasaturo A, Hofmann RM, Friedl P. *Phys Biol*. 2011; 8:015010. [PubMed: 21301056]
31. Kloxin AM, Benton JA, Anseth KS. *Biomaterials*. 2010; 31:1–8. [PubMed: 19788947]
32. Brigham MD, Bick A, Lo E, Bendali A, Burdick JA, Khademhosseini A. *Tissue Eng Part A*. 2009; 15:1645–1653. [PubMed: 19105604]
33. Khetan S, Burdick JA. *Biomaterials*. 2010; 31:8228–8234. [PubMed: 20674004]
34. Guvendiren M, Burdick JA. *Nat Commun*. 2012; 3:792. [PubMed: 22531177]
35. Ridley AJ. *Cell*. 2011; 145:1012–1022. [PubMed: 21703446]
36. Pankov R, Endo Y, Even-Ram S, Araki M, Clark K, Cukierman E, Matsumoto K, Yamada KM. *J Cell Biol*. 2005; 170:793–802. [PubMed: 16129786]
37. Meller J, Vidali L, Schwartz MA. *J Cell Sci*. 2008; 121:1981–1989. [PubMed: 18505794]
38. Chuang YY, Tran NL, Rusk N, Nakada M, Berens ME, Symons M. *Cancer Res*. 2004; 64:8271–8275. [PubMed: 15548694]
39. Chan AY, Coniglio SJ, Chuang YY, Michaelson D, Knaus UG, Philips MR, Symons M. *Oncogene*. 2005; 24:7821–7829. [PubMed: 16027728]
40. Yoon CH, Hyun KH, Kim RK, Lee H, Lim EJ, Chung HY, An S, Park MJ, Suh Y, Kim MJ, Lee SJ. *FEBS Lett*. 2011; 585:2331–2338. [PubMed: 21704033]
41. Gastonguay A, Berg T, Hauser AD, Schuld N, Lorimer E, Williams CL. *Cancer Biol Ther*. 2012; 13:647–656. [PubMed: 22549160]
42. Zanca C, Cozzolino F, Quintavalle C, Di Costanzo S, Ricci-Vitiani L, Santoriello M, Monti M, Pucci P, Condorelli G. *J Cell Physiol*. 2010; 225:63–72. [PubMed: 20648624]
43. O'Connor KL, Mercurio AM. *J Biol Chem*. 2001; 276:47895–47900. [PubMed: 11606581]
44. Baugher PJ, Krishnamoorthy L, Price JE, Dharmawardhane SF. *Breast Cancer Res*. 2005; 7:R965–974. [PubMed: 16280046]
45. Montalvo-Ortiz BL, Castillo-Pichardo L, Hernandez E, Humphries-Bickley T, De la Mota-Peynado A, Cubano LA, Vlaar CP, Dharmawardhane S. *J Biol Chem*. 2012; 287:13228–13238. [PubMed: 22383527]
46. Wu YI, Frey D, Lungu OI, Jaehrig A, Schlichting I, Kuhlman B, Hahn KM. *Nature*. 2009; 461:104–108. [PubMed: 19693014]
47. Yoo SK, Deng Q, Cavnar PJ, Wu YI, Hahn KM, Huttenlocher A. *Dev Cell*. 2010; 18:226–236. [PubMed: 20159593]
48. MacKay JL, Keung AJ, Kumar S. *Biophysical journal*. 2012; 102:434–442. [PubMed: 22325265]

49. Gossen M, Bujard H. *Proc Natl Acad Sci U S A*. 1992; 89:5547–5551. [PubMed: 1319065]
50. Gossen M, Freundlieb S, Bender G, Muller G, Hillen W, Bujard H. *Science*. 1995; 268:1766–1769. [PubMed: 7792603]
51. Fussenegger M, Morris RP, Fux C, Rimann M, von Stockar B, Thompson CJ, Bailey JE. *Nat Biotechnol*. 2000; 18:1203–1208. [PubMed: 11062442]
52. Weber W, Fux C, Daoud-el Baba M, Keller B, Weber CC, Kramer BP, Heinzen C, Aubel D, Bailey JE, Fussenegger M. *Nat Biotechnol*. 2002; 20:901–907. [PubMed: 12205509]
53. Zhao HF, Boyd J, Jolicoeur N, Shen SH. *Hum Gene Ther*. 2003; 14:1619–1629. [PubMed: 14633404]
54. Braselmann S, Graninger P, Busslinger M. *Proc Natl Acad Sci U S A*. 1993; 90:1657–1661. [PubMed: 8446579]
55. Wang Y, O'Malley BW Jr, Tsai SY, O'Malley BW. *Proc Natl Acad Sci U S A*. 1994; 91:8180–8184. [PubMed: 8058776]
56. No D, Yao TP, Evans RM. *Proc Natl Acad Sci U S A*. 1996; 93:3346–3351. [PubMed: 8622939]
57. Wang SY, LaRosa GJ, Gudas LJ. *Dev Biol*. 1985; 107:75–86. [PubMed: 2981185]
58. Hu MC, Davidson N. *Cell*. 1987; 48:555–566. [PubMed: 3028641]
59. Mullick A, Xu Y, Warren R, Koutroumanis M, Guilbault C, Broussau S, Malenfant F, Bourget L, Lamoureux L, Lo R, Caron AW, Pilotte A, Massie B. *BMC Biotechnol*. 2006; 6:43. [PubMed: 17083727]
60. Liu HS, Lee CH, Lee CF, Su IJ, Chang TY. *Biotechniques*. 1998; 24:624–628. 630–622. [PubMed: 9564536]
61. Iniesta AA, Garcia-Heras F, Abellon-Ruiz J, Gallego-Garcia A, Elias-Arnanz M. *J Bacteriol*. 2012; 194:5875–5885. [PubMed: 22923595]
62. Shin KJ, Wall EA, Zavzavadjian JR, Santat LA, Liu J, Hwang JI, Rebres R, Roach T, Seaman W, Simon MI, Fraser ID. *Proc Natl Acad Sci U S A*. 2006; 103:13759–13764. [PubMed: 16945906]
63. Machesky LM, Hall A. *J Cell Biol*. 1997; 138:913–926. [PubMed: 9265656]
64. Ridley AJ, Paterson HF, Johnston CL, Diekmann D, Hall A. *Cell*. 1992; 70:401–410. [PubMed: 1643658]
65. Peltier J, Schaffer DV. *Methods Mol Biol*. 2010; 621:103–116. [PubMed: 20405362]
66. Ulrich TA, Jain A, Tanner K, MacKay JL, Kumar S. *Biomaterials*. 2010; 31:1875–1884. [PubMed: 19926126]
67. Ulrich TA, Lee TG, Shon HK, Moon DW, Kumar S. *Biomaterials*. 2011; 32:5633–5642. [PubMed: 21575987]
68. Ananthanarayanan B, Kim Y, Kumar S. *Biomaterials*. 2011; 32:7913–7923. [PubMed: 21820737]
69. Tamaki M, McDonald W, Amberger VR, Moore E, Del Maestro RF. *J Neurosurg*. 1997; 87:602–609. [PubMed: 9322849]
70. An Z, Gluck CB, Choy ML, Kaufman LJ. *Cancer Lett*. 2010; 292:215–227. [PubMed: 20060208]
71. Yang YL, Motte S, Kaufman LJ. *Biomaterials*. 2010; 31:5678–5688. [PubMed: 20430434]
72. Stein AM, Demuth T, Mobley D, Berens M, Sander LM. *Biophys J*. 2007; 92:356–365. [PubMed: 17040992]
73. Tran NL, McDonough WS, Savitch BA, Fortin SP, Winkles JA, Symons M, Nakada M, Cunliffe HE, Hostetter G, Hoelzinger DB, Rennert JL, Michaelson JS, Burkly LC, Lipinski CA, Loftus JC, Mariani L, Berens ME. *Cancer Res*. 2006; 66:9535–9542. [PubMed: 17018610]
74. Zhang Y, Gazit Z, Pelled G, Gazit D, Vunjak-Novakovic G. *Integr Biol*. 2011; 3:39–47.
75. Lee SS, Horvath P, Pelet S, Hegemann B, Lee LP, Peter M. *Integr Biol*. 2012; 4:381–390.
76. Bennett MR, Pang WL, Ostroff NA, Baumgartner BL, Nayak S, Tsimring LS, Hasty J. *Nature*. 2008; 454:1119–1122. [PubMed: 18668041]
77. Cambridge SB, Geissler D, Keller S, Curten B. *Angew Chem Int Ed Engl*. 2006; 45:2229–2231. [PubMed: 16506298]
78. Sauers DJ, Temburni MK, Biggins JB, Ceo LM, Galileo DS, Koh JT. *ACS Chem Biol*. 2010; 5:313–320. [PubMed: 20050613]

79. Cambridge SB, Geissler D, Calegari F, Anastassiadis K, Hasan MT, Stewart AF, Huttner WB, Hagen V, Bonhoeffer T. *Nat Methods*. 2009; 6:527–531. [PubMed: 19503080]
80. Wosnick JH, Shoichet MS. *Chem Mater*. 2007; 20:55–60.
81. Wylie RG, Ahsan S, Aizawa Y, Maxwell KL, Morshead CM, Shoichet MS. *Nat Mater*. 2011; 10:799–806. [PubMed: 21874004]
82. Kraning-Rush CM, Carey SP, Lampi MC, Reinhart-King CA. *Integr Biol*. 2013; 5:606–616.
83. Lo CM, Wang HB, Dembo M, Wang YL. *Biophys J*. 2000; 79:144–152. [PubMed: 10866943]
84. Saez A, Ghibaud M, Buguin A, Silberzan P, Ladoux B. *Proc Natl Acad Sci U S A*. 2007; 104:8281–8286. [PubMed: 17488828]
85. Suri S, Schmidt CE. *Acta Biomater*. 2009; 5:2385–2397. [PubMed: 19446050]
86. Joshi-Barr S, Karpiak JV, Ner Y, Wen JH, Engler AJ, Almutairi A. *J Vis Exp*. 2013:e50018.
87. Friedl P, Wolf K. *J Cell Biol*. 2010; 188:11–19. [PubMed: 19951899]
88. Friedl P, Alexander S. *Cell*. 2011; 147:992–1009. [PubMed: 22118458]
89. Gaggioli C, Hooper S, Hidalgo-Carcedo C, Grosse R, Marshall JF, Harrington K, Sahai E. *Nat Cell Biol*. 2007; 9:1392–1400. [PubMed: 18037882]
90. Condeelis J, Pollard JW. *Cell*. 2006; 124:263–266. [PubMed: 16439202]
91. Kurosaka S, Kashina A. *Birth Defects Res C Embryo Today*. 2008; 84:102–122. [PubMed: 18546335]
92. Shaw TJ, Martin P. *J Cell Sci*. 2009; 122:3209–3213. [PubMed: 19726630]

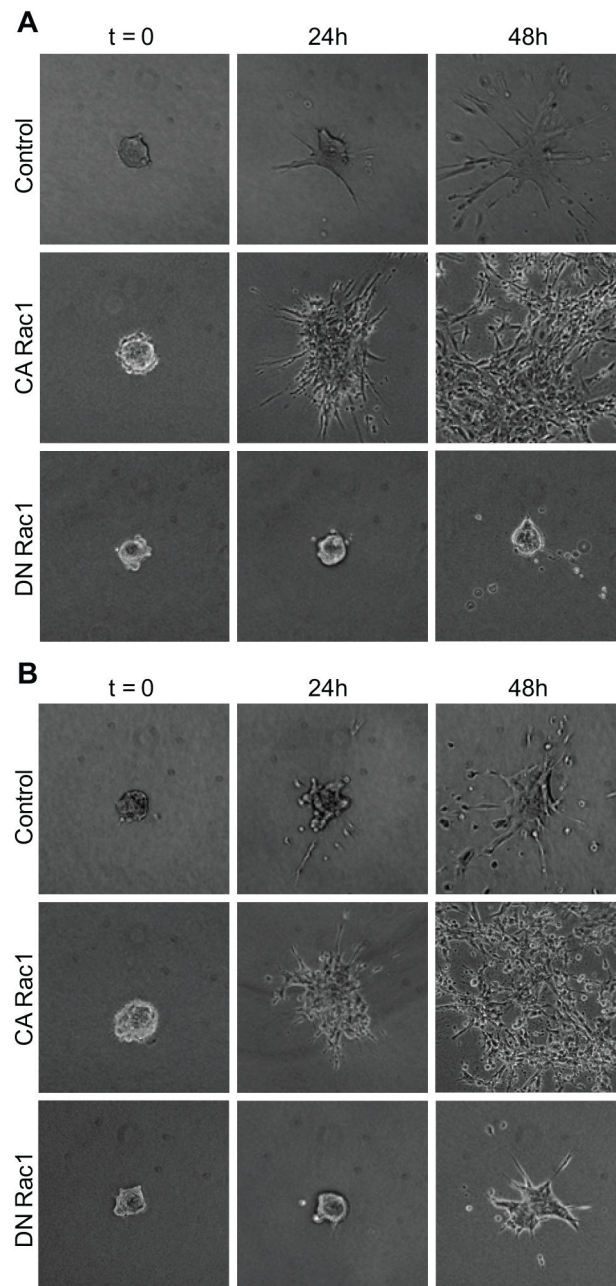


Fig. 1. Direct control over cell migration in 3D matrices through inducible expression of Rac1 GTPase mutants. (A) Cells expressing doxycycline-inducible CA Rac1, DN Rac1, or an empty control vector were cultured as multicellular spheroids in the presence of doxycycline to induce expression, implanted into 1 mg/ml collagen gels still in the presence of doxycycline, and imaged over several days. (B) Cells expressing cumate-inducible CA Rac1, DN Rac1, or a control vector were cultured in the presence of cumate and similarly implanted into 1 mg/ml collagen gels. Scale bar = 100 μ m.

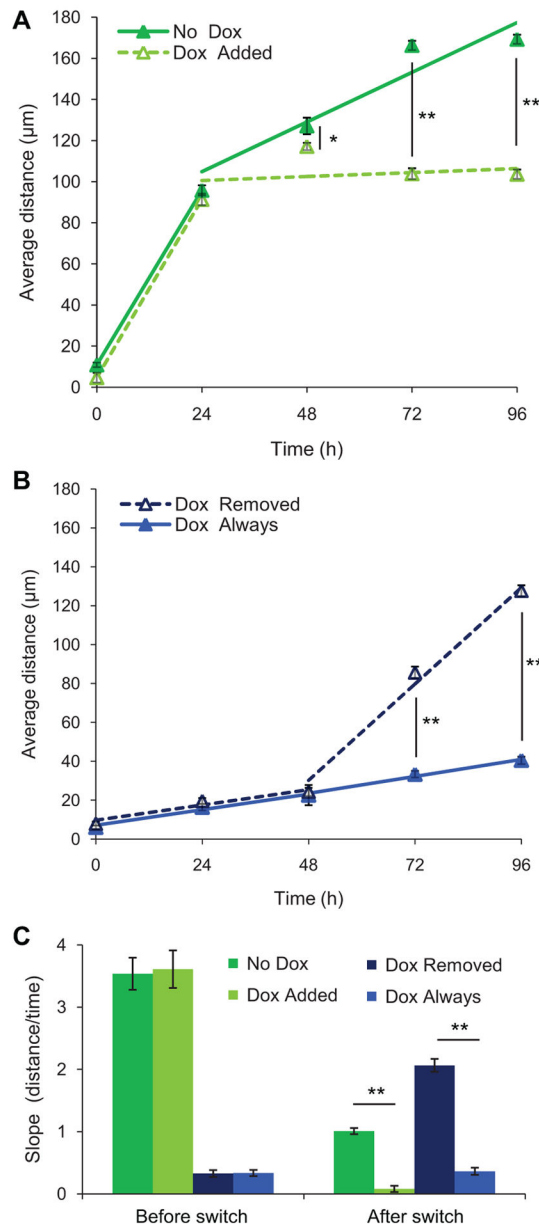
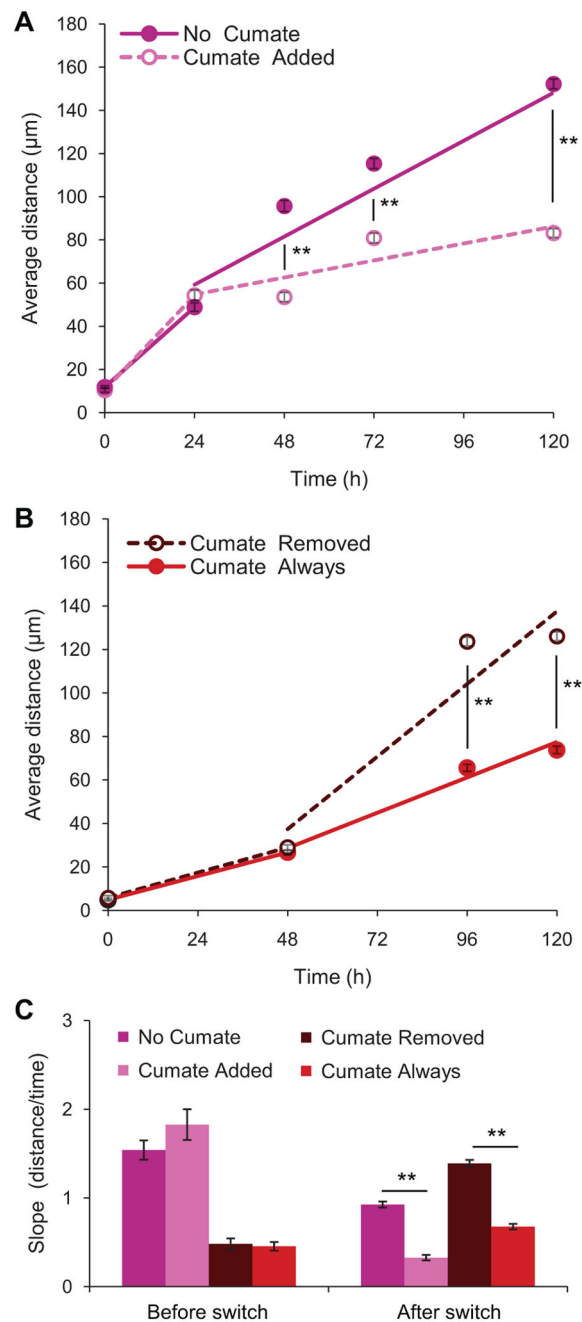


Fig. 2. Dynamically switching expression of doxycycline-inducible DN Rac1 on and off permits temporal control over cell migration. Cells expressing doxycycline-inducible DN Rac1 were cultured as spheroids with or without doxycycline and implanted into 1 mg/ml collagen gels at $t = 0$. Doxycycline was later removed or added, and the distance that cells migrated away from the spheroid edge was measured over time, shown as mean \pm s.e. (A) Spheroids first cultured in the absence of doxycycline were subjected to a medium change 24 hours after implantation to either add doxycycline to induce DN Rac1 expression (“Dox Added”, $n = 71$ – 723 cells from 29 spheroids in total) or remain without doxycycline (“No Dox”, $n = 82$ – 1302 cells from 32 spheroids in total). (B) Spheroids first cultured in the presence of doxycycline to induce DN Rac1 expression were subjected to a medium change 48 hours

after implantation to either remove doxycycline to turn off DN Rac1 expression (“Dox Removed”, $n = 107\text{--}623$ cells from 38 spheroids in total) or remain with doxycycline (“Dox Always”, $n = 121\text{--}486$ cells from 43 spheroids in total). Linear fits were calculated separately for data points before and after the medium changes. (C) Slopes for each fit in A and B; error bars are s.e. of the slope. * denotes $p < 0.05$ and ** denotes $p \ll 0.001$ (t-test).

**Fig. 3.**

Dynamic switching of cumate-inducible DN Rac1 permits similar temporal control over cell migration. Cells expressing cumate-inducible DN Rac1 were cultured as spheroids with or without cumate and implanted into 1 mg/ml collagen gels at $t = 0$. Cumate was later removed or added, and the distance that cells migrated away from the spheroid edge was measured over time, shown as mean \pm s.e. (A) Spheroids first cultured in the absence of cumate were subjected to a medium change 24 hours after implantation to either add cumate to induce DN Rac1 expression (“Cumate Added”, $n = 95$ –561 cells from 18 spheroids in total) or remain without cumate (“No Cumate”, $n = 220$ –993 cells from 40 spheroids in

total). (B) Spheroids first cultured in the presence of cumate to induce DN Rac1 expression were subjected to a medium change 48 hours after implantation to either remove cumate to turn off DN Rac1 expression (“Cumate Removed”, $n = 144\text{--}1115$ cells from 40 spheroids in total) or remain with cumate (“Cumate Always”, $n = 150\text{--}874$ cells from 43 spheroids in total). Linear fits were calculated separately for data points before and after the medium changes. (C) Slopes for each fit in A and B; error bars are s.e. of the slope. * denotes $p < 0.05$ and ** denotes $p \ll 0.001$ (t-test).

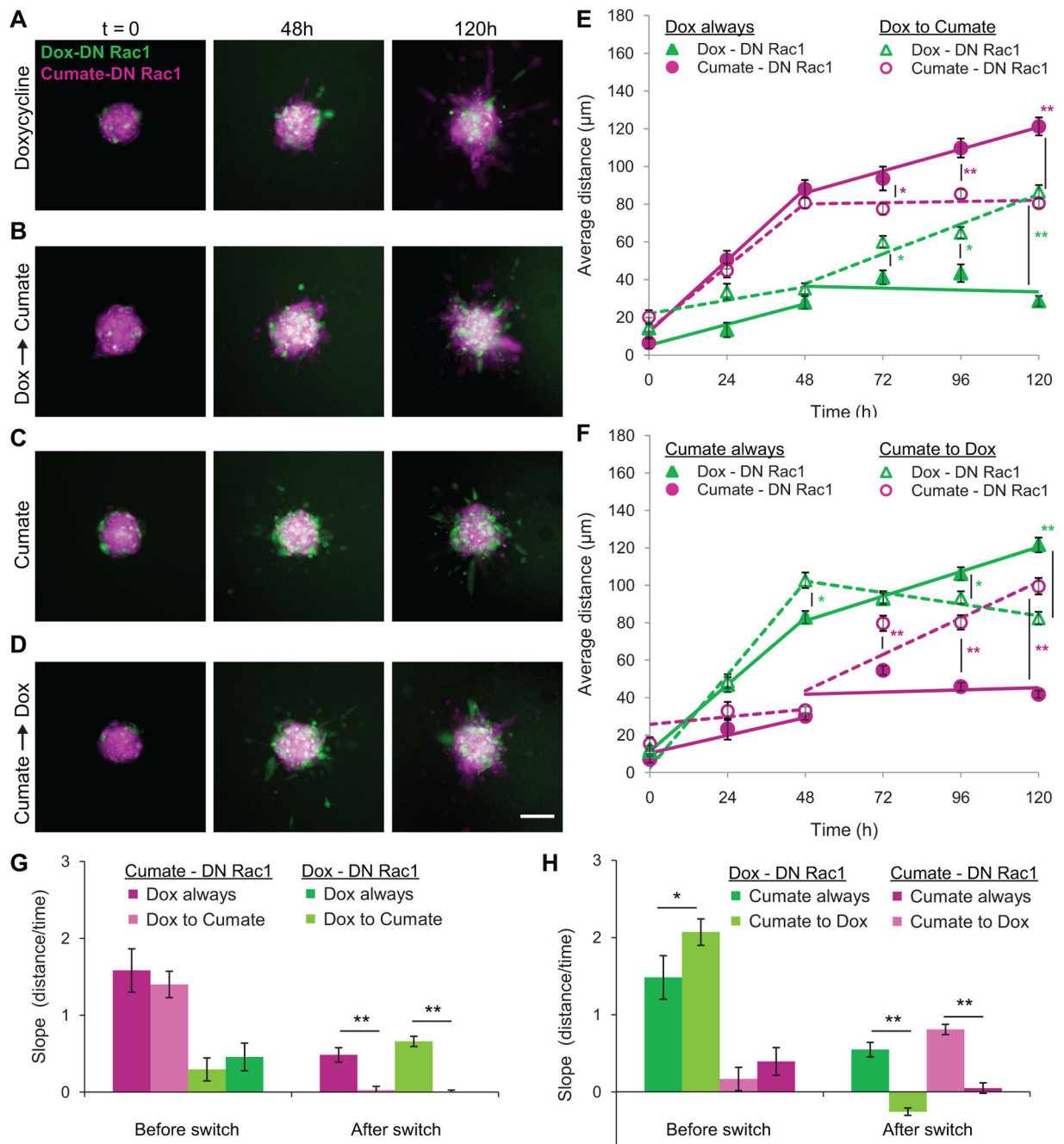


Fig. 4. Mixed populations of cells can be spatially patterned through orthogonal control over the migration of each subpopulation. Cells expressing doxycycline-inducible DN Rac1 (“Dox - DN Rac1”, green) and cells expressing cumate-inducible DN Rac1 (“Cumate - DN Rac1”, magenta) were co-cultured as heterogeneous spheroids in either doxycycline or cumate and implanted into 1 mg/ml collagen gels at $t = 0$. (A) Spheroids cultured in the presence of doxycycline to suppress the migration of doxycycline-inducible DN Rac1 cells. (B) Spheroids first cultured in the presence of doxycycline and then subjected to a medium

change at $t = 48$ h to remove doxycycline and add cumate. (C) Spheroids cultured in the presence of cumate to suppress the migration of cumate-inducible DN Rac1 cells. (D) Spheroids first cultured in the presence of cumate and then subjected to a media change at $t = 48$ h to remove cumate and add doxycycline. For (A–D), the epifluorescence images are overlays of 9–34 spheroids; scale bar = 100 μm . (E) Cell migration was quantified as the average distance that cells had migrated away from the spheroids for the conditions shown in A ($n = 19$ –162 cells from 9 spheroids in total) and B ($n = 14$ –361 cells from 34 spheroids in total). (F) Average cell migration distances for the spheroids shown in C ($n = 14$ –324 cells from 27 spheroids in total) and D ($n = 16$ –213 cells from 24 spheroids in total). Linear fits were calculated separately for the data points before and after the media changes. (G) Slopes for each fit in E. (H) Slopes for each fit in F. All error bars are s.e. * denotes $p < 0.05$ and ** denotes $p \ll 0.001$ (t-test).